Review

Porous gold nanoparticles: thermal stability, optical response and support-free synthesis

Laura Juhász [1], Zoltán Erdélyi [1] and Csaba Cserháti [1]

[1] Department of Solid State Physics, Faculty of Science and Technology, University of Debrecen, P.O. Box. 400, Debrecen, H-4002, Hungary;

* Correspondence: e-mail@e-mail.com; Tel.: (optional; include country code; if there are multiple corresponding authors, add author initials) +xx-xxxx-xxx-xxxx (F.L.)

Abstract: 3D metal nanostructures are often the basis of several applications such as in catalysis, plasmonics, medical diagnosis, therapy, drug screening, ophthalmologic, and biomedical applications. Porous gold nanoparticles (PGNs) are intensively investigated due to their outstanding morphological as well as advantageous optical properties. Unfortunately, the thermal stability of these open-porous structures is poor, i.e. even as a result of low-temperature annealing (150°C in air), their porosity disappears and they lose their favorable optical properties. In order to preserve their beneficial properties, a thin metal oxide coating can be applied. Changing the coating's thickness and/or composition, the optical response of the PGNs can also be tuned in a wide wavelength region. Moreover, these nanoparticles can be synthesized also in support-free form, which makes them more attractive from an application point of view. This review article summarizes some of the preparation modes of these complex nanostructures (fixed and support-free), as well as their thermal stability and optical responses.

Keywords: porous gold nanoparticles, plasmons, optical absorption, dewetting, dealloying, support-free nanoparticles

1. Introduction

Nanomaterials show significantly different mechanical, optical, electrical, and chemical properties than their bulk counterparts. The main concept of nanomaterials is that their size is limited between 1 and 100 nm in at least one of their dimensions. The applications of nanomaterials have a long history, in spite of the fact that the mechanism and the reason for their interesting properties were still intact and undiscovered for a long time: PbS nanostructure has been applied as a hair dyeing technology by the Ancient Egyptian [1], furthermore, the unique optical properties of the 4th century roman Lycurgus cup also come from the presence of gold-silver nanoparticles in their main matrix [2]. Technological developments, e.g. the appearance of electron – and atomic microscopes, as well as the improvement of fabrication methods lead to a better understanding of nanomaterials and their direct and targeted production became notable.

Metal nanoparticles are the frontiers of nanostructures in several applications such as in biomedical application [3–5], phototherapy [6–9], imaging [10,11], drug delivery [12,13], biosensor [14]. The main aspect of their usage is that they exhibit outstanding optical response, i.e. they show a great absorption peak in the visible region. Metal nanoparticles also have great antibacterial activity, which makes them a promising candidate in nanomedicine technology [15]. The reason for their excellent optical properties was explained in 1908 by Gustav Mie, who theorised this behaviour for spherical particles based on Maxwell's equations [16]. When light interacts with metal nanoparticles, the electron in its conductive band starts to oscillate in a collective way and the quantum of the oscillation is the so-called plasmon. The electrons are localised in the nanoparticles, resulting in a so-called localised surface plasmon resonance (LSPR). This property gives rise to sharp absorption peaks in

Preprints (www.preprints.org) | NOT PEER-REVIEWED | Posted: 5 June 2023 doi:10.20944/preprints202306.0324.v1

the optical spectrum and strong electromagnetic near-field enhancements. The size and shape of the nanoparticles as well as their surrounding medium have a high impact on its optical response [17]. Porous gold nanoparticles have greater plasmonic properties than their solid counterparts, i.e. the dipole plasmon peak appears in the near-infrared region, which broadens the applicability of PGNs for instance in biosensors, catalysis, plasmonics, medical diagnosis, therapy, drug screening, ophthalmologic devices. Hu et. al. reported a method using near-infrared light to heat hollow porous gold nanoparticles for thermal decomposition of NH_4HCO_3 [18].

The fabrication of porous nanoparticles can happen in several ways such as ambient wet-chemical method [19], nanoimprint lithography[20], one-step solution phase method at room temperature[21], laser-induced process [22], however, the most common and precise way to prepare porous gold nanoparticles is the dewetting-dealloying procedure. Wang et al. were the first to prepare porous gold nanoparticles using these two methods over a wide diameter range [23].

In this review article, we present a method for the preparation of porous gold nanoparticles by the dewetting-dealloying method based on the literature results. The thermal stability of PGN is one of the most important issues for its applicability, and we summarize the thermal properties as well as the possibilities to stabilize the morphology up to high temperatures. We also show how the optical properties of this unique nanostructure can be tuned over a wide wavelength range, extending its applicability. Finally, we will demonstrate a method for the support-free synthesis of porous gold nanoparticles in water. The method may have good potential for biomedical applications.

2. Dewetting-dealloying

Thompson et.al. described the mechanism of dewetting in 2012 and they stated when the heat treatment of a thin film occurs, the thin films develop into islands or nanoparticles due to the metastable state of the film after deposition [24]. The temperature of the dewetting process is not necessarily higher than the melting point of the material, i.e. the phenomenon takes place in the solid state. In general, dewetting consists of three steps: i) hole formation of thin film, ii) which is followed by the increasing of the hole iii) till the films break into islands. Several properties of the thin films have a high impact on the dewetting process (thickness, grain size, temperature etc.). Thickness and temperature have a strong influence on the speed of the dewetting, for instance, hole formation is easier in thinner films. The main driving force of dewetting is the minimization of energy, i.e. the system is forced to decrease the total energy of the free surfaces between the film and substrate as well as between the film-substrate interface.

The most common example of dewetting is the fabrication Au-Ag alloy nanoparticles on a substrate material. In that case, gold and silver thin films are deposited on the surface of the substrate material from a high-purity material. Afterward, the sample is annealed at high temperature (from 200°C to 1000°C) in an inert gas atmosphere (Ar, Ar+H_2, N_2) for the desired time. As a result of the dewetting, nanoparticles of Au-Ag alloy form on the surface of the substrate. The properties of these nanoparticles strongly depend on the initial thickness and the condition of the heat treatment. This fact gives the opportunity to vary the diameter of nanoparticles only by manipulating the initial thickness of the bilayer.

To reach a porous gold structure, dealloying process is used in general. During this process, the selective etching of silver occurs and as a consequence porous gold nanostructure form. Dealloying is when one or more component is selectively dissolved from a homogeneous alloy. The alloy and the etching solvent react with each other and the more noble metal is able to move freely along the interface between the solving medium and the alloy during the dissolution of the less noble component. However, the composition of the initial alloy is a crucial point in terms of the process. Finally, the remaining component rebuilds a new 3D open porous structure [25]. In the case of Au-Ag nanoparticles, silver is selectively etched from the alloy nanoparticles using nitric acid. The time, the temperature, and the concentration of HNO_3 can drastically alter the morphology of PGNs. Figure 1.

Preprints (www.preprints.org) | NOT PEER-REVIEWED | Posted: 5 June 2023 doi:10.20944/preprints202306.0324.v1

shows schematically the dewetting and dealloying procedures in the fabrication of porous gold nanoparticles.

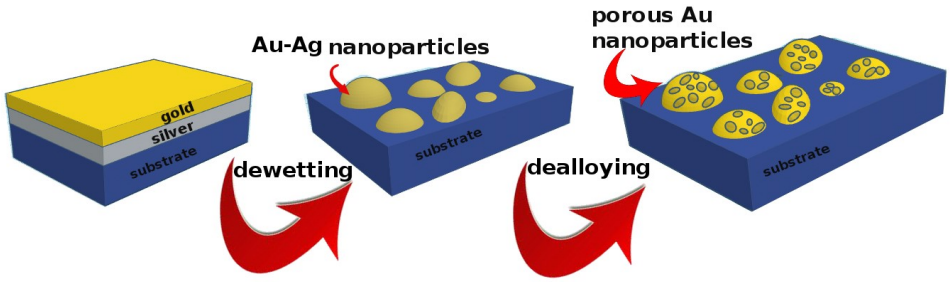

Figure 1. Illustration of dewetting and dealloying procedures

3. Thermal stability

The thermal stability of porous gold is a major area of interest within the field of applications and has been intensively studied in the last years. Kosinova et.al reported the fabrication of PGNs and their low thermal stability [26]. They demonstrated the formation of doughnut-like gold nanoparticles using thermal coarsening. In their work, PGNs with a diameter ranging from 100 to 500 nm were successfully fabricated on SiO_2/Si substrate using the dewetting-dealloying method. Unfortunately, this 3D structure lost its original morphology even after low-temperature (150°C) annealing in air and vacuum that was characterized using high-resolution scanning electron microscopy (HR-SEM). Figure 2. shows HR-SEM images of PGNs as-dealloyed and annealed in vacuum for half an hour from [26,27]. The development of doughnut-like nanoparticles is controlled by diffusion processes of thermal coarsening. They found that the optimal temperature is 350°C and approximately one hour of annealing in air. Not only an experimental but also a qualitative 2D model of PGNs thermal coarsening was presented and it was illustrated that the higher positive average surface curvature in the near-surface regions compared with the outer parts of PGNs causes the closure of the originally opened porous structure. They also have shown that the annealing atmosphere has a high impact on the formation of the microstructural evolution of PGNs, and as a consequence, PGNs show higher thermal stability during annealing in a vacuum. In this work, a successful and simple transition method from open to close porosity of PGNs is reported using diffusion-controlled processes.

However, the thermal stability of PGNs is a crucial property for the application. It is well-known that porous metals are promising candidates for sensors, or biomedical applications [28], but this thermal instability limits their utilization for instance in high-temperature applications.

According to Biener et.al., a few nanometers thick alumina or titania layer can stabilize and functionalize the structure of nanoporous metals [29]. It was demonstrated that even only 1 nm ALD deposited alumina films can stabilize the nanoscale morphology of disk-shaped samples of porous gold up to 1000°C, as well as its mechanical properties (such as stiffness, hardness) have improved due to the covering layer. Titania covering was also the focus of their work, and it was found that the titania layer is also appropriate to stabilize the porous structure up to high temperatures. On the other hand, the titania covering layer gives an outstanding catalytic activity for the titania-coated porous gold nanoparticles (TPGNs). Even so, pristine TiO_2/Au film is catalytically in-active for CO oxidation, however, after 600°C heat-treatment the coated porous gold film become more active than the as-prepared one. Jia and co-workers also investigated the catalytic activity of titania-coated porous gold electrodes fabricated wet chemical methods and reported a remarkable activity during methanol photoelectrocatalytic reactions [30]. Atta et.al has developed titania on gold nanostars by a simple hydrothermal route, and highlighted the fact that LSPR bands of titania-coated gold nanostars absorb the near-infrared radiation and at the same time significantly enhance the H_2 evolution [31]. Findings in [29–31] are in

Preprints (www.preprints.org) | NOT PEER-REVIEWED | Posted: 5 June 2023 doi:10.20944/preprints202306.0324.v1

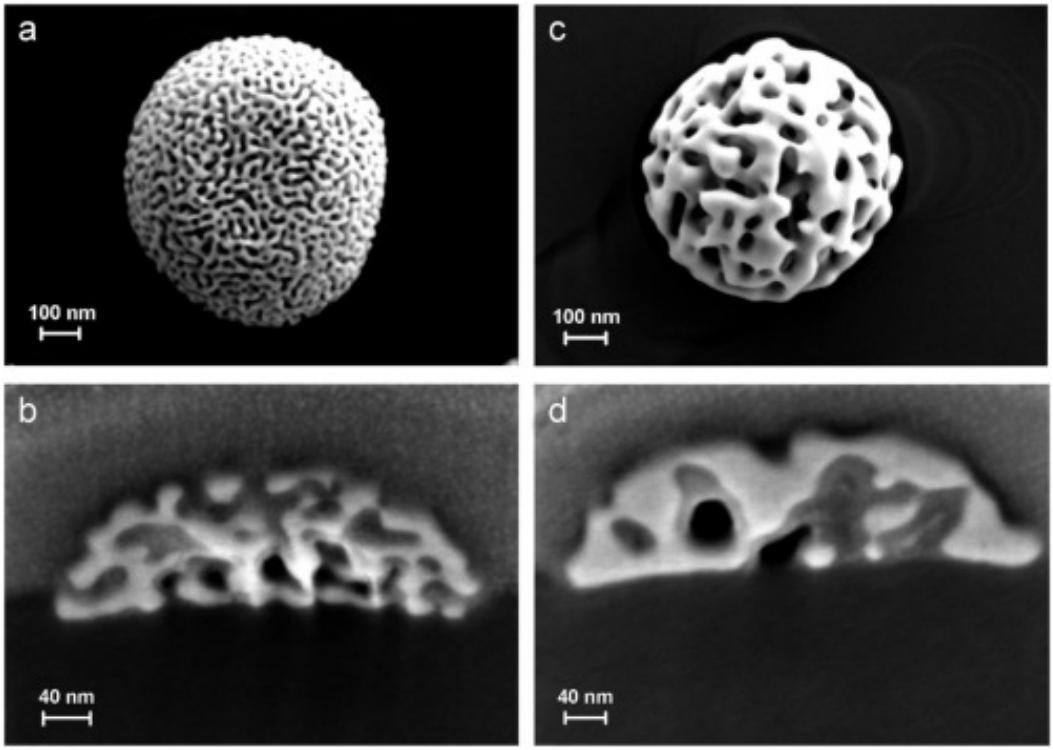

Figure 2. (a, c) Top view and (b, d) cross-sectional SEM images of PGNs: (a, b) as-dealloyed and (c, d) annealed in vacuum for 30 min. (Reprinted from Fabrication of hollow gold nanoparticles by dewetting, dealloying and coarsening, Volume 102, Acta Materialia [26])

good agreement with the crystallography changes of titania coating at this temperature range. It is well-known that ALD-deposited titania is amorphous up to 150°C deposition temperature [32], and this fact is directly in line with the low catalytic activity of ALD deposited pristine TiO_2 [30,33,34].

As far as PGNs thermal stability is concerned, Kosinova et.al demonstrated that a few nanometer thick alumina coating can passivate the surface of PGNs as well as preserve the morphology of PGNs up to high temperature (900°C) [35]. To cover the PGNs evenly and uniformly with Al_2O_3, they used the plasma-enhanced atomic layer deposition (PE-ALD) method due to its low deposition temperature, which hinders the diffusion of gold during the deposition. Alumina-coated porous gold nanoparticle (APGN) samples were annealed at different temperatures from 350°C to 900°C in air for an hour and changes in the morphology were observed using SEM. Up to 600 °C the structure of APGNs was stable, however, above this temperature dark and light parts appeared on the surface of the APGNs in the SEM images. The dark parts are poor in gold, which indicates that the slow diffusion of gold started during the annealing at this temperature. After high-temperature annealing, solid, faceted gold nanoparticles formed and left behind an empty alumina shell. Due to the difference between the thermal expansion coefficients of gold and alumina, the covering layer becomes fragmented, which gives the opportunity for gold to diffuse out on the surface of the alumina shell. The main driving force is to reduce the total energy of all surfaces and interfaces in the system.

TPGNs were also the subject of studies in terms of thermal stability [36]. Covering of TPGNs was performed using ALD and TPGNs samples were annealed under the same conditions as in Kosinova's work. Similarities were reported with the findings of Biener et. al., i.e. titania coating can preserve the morphology of PGNs up to 600°C and its morphology is unchanged up to 600°C. However, dark and light parts appear on the surface of TPGNs in the SEM images above this temperature. This also corresponds to the findings of Kosinova et.al. [35]. Annealing the TPGNs above 800°C their structure changes

Preprints (www.preprints.org) | NOT PEER-REVIEWED | Posted: 5 June 2023 doi:10.20944/preprints202306.0324.v1

dramatically; the gold forms a solid, spherical particle, which is covered by a titania layer, forming a core-shell structure. The authors presented the following scenario which takes place between the low and high-temperature states. Close to the melted state of gold, due to its high surface diffusivity, the gold atoms diffuse inward, forming a nano-sphere, pushing the rutile flakes – which evolve due to the allotropic phase transformation – outward, to the surface of the gold particle. The allotropic phase transition of titania was confirmed using electron diffraction. The driving force for this process presumably is to reduce the total TiO_2/Au interface as much as possible. The key is that this process can only start after the titania coating layer starts to transform into the rutile phase.

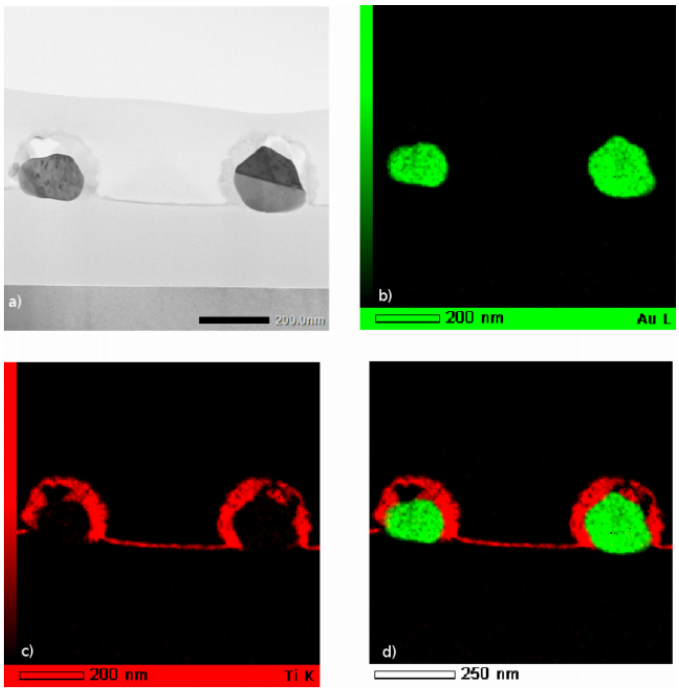

Figure 3. (a) Cross-section view of TPGNs by FIB and imaged TEM/EDS after annealing 900°C for an hour. The porous structure of the gold totally disappeared and collapsed completely into a solid sphere. Note that Au sphere on the right in figure. (b) Au elemental distribution, (c) Ti elemental distribution, and (d) Au and Ti distribution. (Reprinted from [36] , with the permission of AIP Publishing.)

4. Optical response (LSPR)

Metal nanoparticles are often used in different applications, such as in sensors, catalyst, cancer therapy, environment protection etc. [37–44]. One of the biggest advantages of this nanostructures is the localized plasmon resonance (LSPR), i.e the free electrons in their conduction electron band interact with the incoming light and oscillate. The quantum of the oscillation is the so-called plasmon. The resonance frequency can be controlled and modified by the shape, size and spacing of the nanoparticles (or nanostars, nanorods). Porosity complicates the interpretation of PGNs extinction properties, which leads to more enhanced plasmonic properties than in the case of solid NPs, i.e. plasmon resonance band can be shifted from the visible to the near-infrared range, which makes an appropriate candidate for example in skin cancer therapy [43–45]. The exact mechanism and theory of the LSPRs in PGNs are thoroughly described and detailed in the literature [38,46,47].

Optical response of solid and porous gold nanoparticles can be drastically different from each other due to the porosity. To prove this fact, Wenye et. al [48] fabricated solid silver-gold alloy and porous gold nanoparticles with controlled particle size using the combination of dewetting and subsequent dealloying procedures. Extinction spectra of

Preprints (www.preprints.org) | NOT PEER-REVIEWED | Posted: 5 June 2023 doi:10.20944/preprints202306.0324.v1

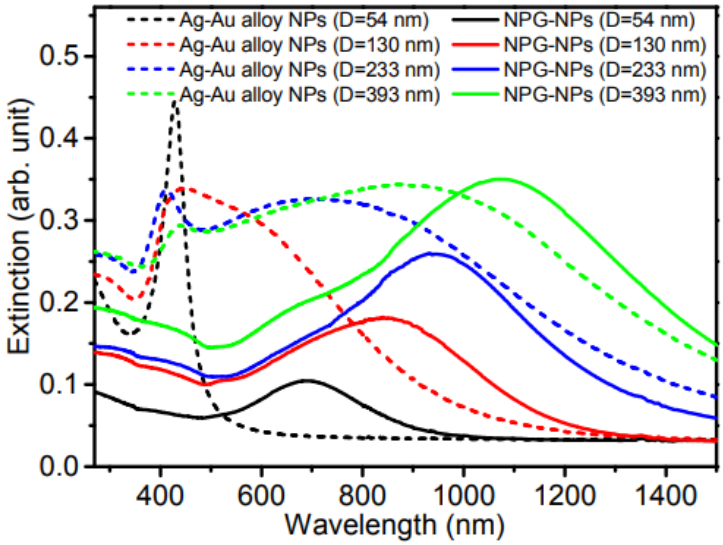

Figure 4. Extinction spectra of solid silver-gold alloy nanoparticles (dashed lines) and porous gold nanoparticles (continuous line). The same color corresponds same average diameter of particles. What can be clearly seen in this figure is the difference between solid alloys and porous gold nanoparticles. Another interesting note is that the porosity also shifts the plasmon peak to the infrared region (Reprinted with permission from [48] Copyright 2017 American Chemical Society.)

solid silver gold and porous gold nanoparticles were measured from 350 nm to 1500 nm. Different sizes of nanoparticles were investigated in their work, however, the porosity of PGN was fixed

Figure 4 shows the measured absorption spectra of silver-gold alloy and porous gold nanoparticles with an average diameter from 54 to 393 nm. It is clearly seen that the position of the plasmon peaks shifts into the red direction with the increase of the average diameter in both cases [48]. One can see that the appearance of the porosity also leads to a red shift of the plasmon peaks. (Compare the dashed line with the same color and a continuous one to see the shift.)

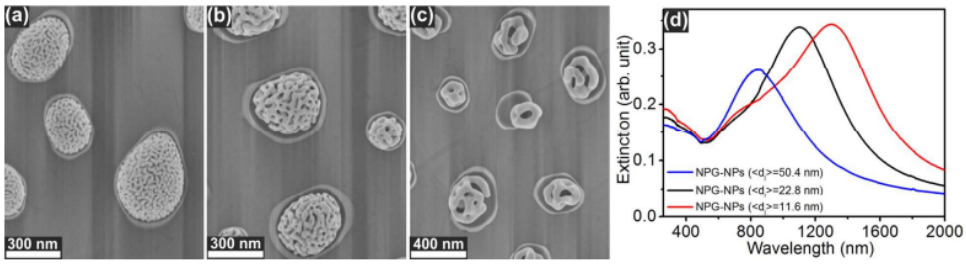

Figure 5. (a), (b) and (c) SEM images show porous gold nanoparticles with different pore size distribution. Corresponding extinction spectra are plotted in (d) diagram Reprinted with permission from [48] Copyright 2017 American Chemical Society.

Wenye et.al. prepared PGNs with different porosity and the optical extinction spectra were measured and the result is presented in Figure 5. It reveals that there has been a significant shift in the position of the dipole plasmon peak, which corresponds with the size of the pores, i.e. the larger the pore size, the larger the shift to the infrared region.

Preprints (www.preprints.org) | NOT PEER-REVIEWED | Posted: 5 June 2023 doi:10.20944/preprints202306.0324.v1

Not only the effect of pore size but also the effect of a thin Al_2O_3 covering layer have been investigated by Wenye et.al. Figure 6 shows the optical response of pristine, 5 nm, and 10 nm alumina-coated PGN, however, the pore size of PGN was fixed. Comparing the black line with blue and red ones it is clearly seen that the dipole plasmon peak position has shifted $\sim$ 150 nm to the red direction. This shift is caused due to the change in the local refractive index surrounding the nanoparticles.

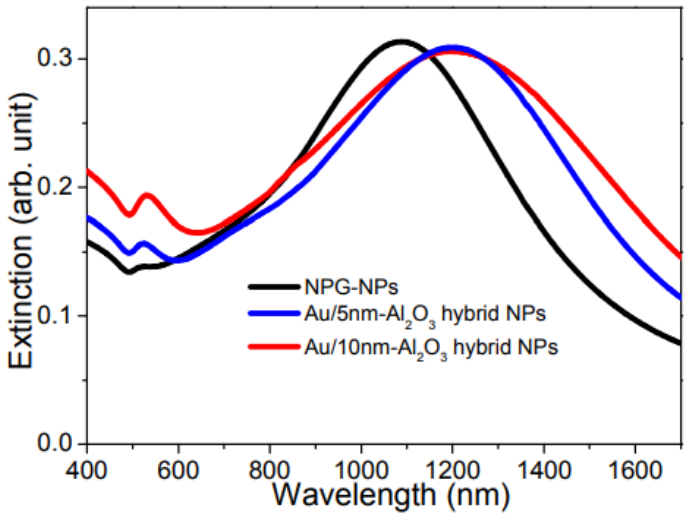

Figure 6. Extinction spectra of PGN and APGN are shown. Comparing the black line with blue and red ones is clearly shown the effect of the covering layer, which is an approximately 150 nm red-shift in the position of dipole plasmon peak. (Reprinted with permission from [48] Copyright 2017 American Chemical Society.)

The optical response of TPGN was also investigated [36]. It is well-known that titania has a much greater ($\sim$2.3) refractive index than alumina ($\sim$1.6). As a consequence, coating PGN with titania gives a significantly higher red-shift ($\sim$400 nm) of the dipole plasmon peak. The optical properties of this hybrid TPGN were measured after heat treatment. It was found that the optical absorption spectra do not change due to heat treatment up to 700°C, however, above this temperature the position of the dipole plasmon peak started to shift to the shorter wavelength. As far as the morphological properties are concerned after this step, slow diffusion of gold was observed. Annealing at higher temperatures, the position of the dipole plasmon peak has shifted in the visible range. As for the morphology, it has drastically changed, i.e. solid gold nanoparticles covered with a thick layer of titanium dioxide were formed on the substrate surface due to the phase transformation of titanium dioxide. These two things together explain the change of the extinction spectra. First, the dipole plasmon peak position of solid gold nanoparticles is located in the visible region, however, the thick titania layer, which covers it, affects a slight red-shift in the position of this peak.

With these experiments, it has been shown that the optical properties of porous gold nanoparticles can be tuned in a controllable way over a wide range of wavelengths by proper annealing conditions than by changing the interparticle distance, the size, and the porosity of the PGNs.

From an application point of view, the stability of these tuned TPGN nanostructures is also important and expected to be enhanced. Indeed, no change was observed in the peak position of samples previously treated at high temperatures following annealing at 750C.

Another opportunity to tune the optical response of PGN is to change the local refractive index of its surrounding medium. As it was shown by Kosinova et. al, and

Preprints (www.preprints.org) | NOT PEER-REVIEWED | Posted: 5 June 2023 doi:10.20944/preprints202306.0324.v1

Wenye et.al, alumina coating causes a 150 nm red-shift. In the case of titania coating, this shift increases up to 400 nm due to the high refractive index of TiO_2 (∼2.3). Using a mixture of Al_2O_3 and TiO_2 as ring layer, the optical response of PGN can be tuned in a controlled and continuous way, because the refractive index of the covering layer can be modified by the ratio of the two different metal-oxides [49].

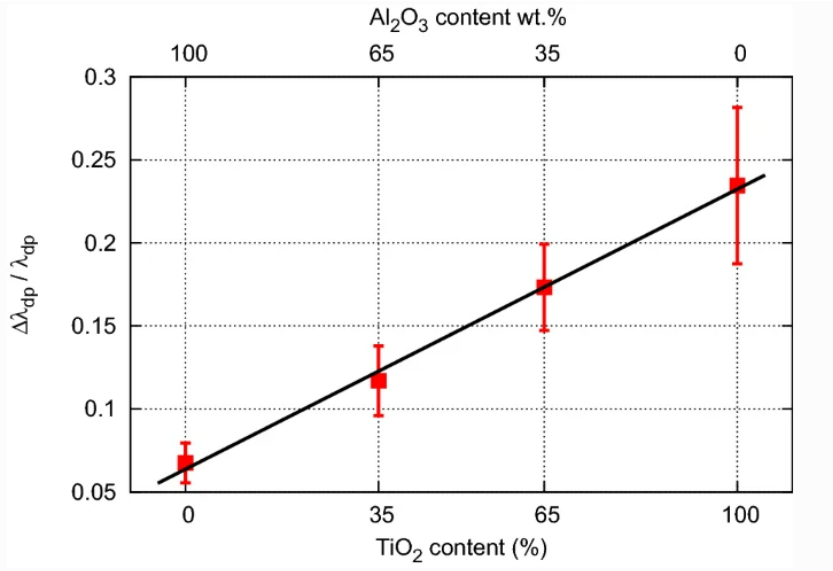

Figure 7. Relative position of dipole plasmon peak of mixed-oxide coated PGNs with different ratio of Al_2O_3/TiO_2. It can clearly see that the higher the content of titania, the higher shift of the dipole plasmon peak to the red. Reprinted from [49], with the permission of Springer Nature.

Relative dipole plasmon peak's position of mixed oxide coated PGNs are plotted in Figure 7. The plot clearly shows that the higher the titania content of the covering layer, the higher the red-shift in the position of the dipole plasmon peak. These findings are in good accordance with the refractive indices of the mixed metal-oxide layers which were measured [49].

Due to the preparation method, PGNs are usually fixed on a solid substrate. PGNs produced in suspension could dramatically widen their application.

To achieve this, Juhász et. al. deposited thin gold-silver layers on CaF_2 substrates, and the bilayer structure was heat treated at 850°C in argon flow for half an hour to perform the dewetting process. [50] The next step was the dealloying of silver, which was combined with the removal of PGNs from the substrate material. The CaF_2 substrate is appropriate for high-temperature annealing during the dewetting step, however, it easily reacts with the nitric acid at room temperature and as a result, PGNs can be detached from the substrate in the dealloying step. The liquid containing the detached PGNs was centrifugated and suspended using deionized water. Since PGNs are separated and deposited simultaneously, this method is called the 1-step method. A so-called two-step method was also developed. Here the PGNs have been fabricated in the dewetting-dealloying process on the Si/SiO_2 substrate with the previously described method. Hydrofluoric acid was applied to remove PGNs from the substrate, which was followed by two-step centrifugation and suspension in deionized water as well.

Samples were analyzed using an inductively coupled plasma optical emission spectrometer to estimate the quantity of PGNs in the solution. It was found that approximately 70% of the amount of gold was detached and suspended after the 2-step centrifugation. Dynamic light scattering (DLS) was used to measure the particle size in aqueous solution. DLS measurements showed a significant increase in the PGN's diameter. The larger mean size of suspended particles after centrifugation was explained by the principle of DLS measurements, i.e. the system detects the hydrodynamic radius of the suspended PGNs,

Preprints (www.preprints.org) | NOT PEER-REVIEWED | Posted: 5 June 2023 doi:10.20944/preprints202306.0324.v1

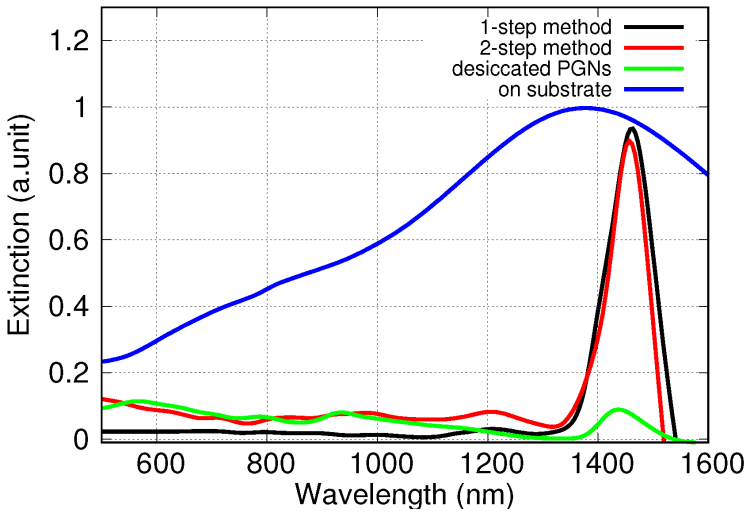

Figure 8. Extinction spectra of PGN in suspension and on substrate are shown in this figure. The blue line corresponds to the absorption of PGN on substrate. Black and red lines show the optical response of PGN in water. The difference between the blue and black/red line is indisputable: the half-width of the absorption spectra in the case of suspension is much narrower, which makes PGN in suspension greater in the application's point of view.[50]

and it is naturally larger than its physical size, which was calculated using scanning electron microscopy images.

Another optional explanation for the increase in the mean particle size is the aggregation of the particles and a small alteration in the shape of the particles due to centrifugation steps. The morphology as well as the optical response of the support-free particles have been checked. As a consequence of the treatment, the optical response of PGN has significantly changed. Figure 8. shows the extinction spectra of the PGNs suspended in water and fixed to the substrate. The blue line corresponding to PGN on the substrate, the black and red lines show the optical response of PGN in suspension. It must be pointed out that the half-width of suspended PGNs is much narrower (compare the black/red lines to the blue one). The centrifugation step has a strong effect on the size distribution and/or the morphology of the PGNs. As a consequence, the mean particle size of the detached PGNs is significantly larger which causes their size distribution to be significantly narrower than on the substrate. To check this, the immobilized PGNs were desiccated on sapphire and investigated by SEM. The green line indicates the appropriate optical response. It is clearly seen that the position of the plasmon peak does not change in the near-infrared region, while its intensity has drastically decreased due to the low amount of desiccated PGNs.

5. Conclusion and Future

In this review article, the outstanding properties of porous gold nanoparticles have been reported. Porous gold nanoparticles have excellent optical properties because they have a great extinction in the infrared region. However, they are thermally very unstable. They found that these nanoparticles lose their porous structure after annealing at low temperatures (150°C) in different atmospheres. To overcome this disadvantage, coating the nanostructure with a few nanometres thick metal oxide layer can stabilize the PGNs until high-temperature annealing. It was shown that alumina-coated PGNs are stable up to 1000°C, while titania-coated PGNs remain intact up to 700°C. Above 700°C, the phase transformation of titanium dioxide occurs and the layer of a few nanometers thick cannot protect the porous structure of the PGNs, resulting in slow diffusion of gold. Further increase in temperature (800°C) causes the titanium dioxide layer to crack into tiny flakes, and the gold, transforming into solid nanoparticles (nanospheres), pushes the titanium dioxide flakes onto the nanoparticle surface. As a result, the porous nanoparticle

is transformed into a solid particle coated with a thick layer of titanium dioxide. This strongly influences its extinction spectrum. i.e. after heat treatment, the plasmon peak is shifted from the near-infrared to the visible range. Based on this property, it is possible to tune the optical response of PGNs over a wide wavelength range by appropriate thermal treatment.

Another way of adjusting the optical extinction of PGNs is to vary the local refractive index of the surrounding medium in a controlled way. The fact that alumina produces a 150 nm redshift and titanium dioxide a 400 nm red-shift in the dipole plasmon peak offers a great opportunity to tune the plasmon peak position in this range using a mixture of the two metal oxides. It was proved that the higher the titania content of the coating layer, the higher the red-shift of the relative dipole plasmon peak's position.

In the dewetting-dealloying process nanoparticles are fabricated in immobilized form on a substrate material. To broaden their application potential, two new methods to synthesize them in water were developed. In the one-step method, CaF_2 was used as a substrate material. During the dealloying process with nitric acid, the acid also detaches the nanoparticles from the substrate. In the case of the two-step method dilute solution of HF was used to detach the dealloyed porous gold nanoparticles from the Si/SiO_2 substrate. In both cases, centrifugation was used to separate the nanoparticles from the acidic medium, after which the PGNs were suspended in water. It has been shown that PGNs also exhibit high plasmonic properties after deposition, i.e. the absorption peak is in the near-infrared region. The half-width of the peak is significantly reduced for the deposited particles compared to PGNs on the substrate, which can be explained by a change in size distribution and/or morphology.

Porous gold nanoparticles can find a wide range of applications from catalyst to biomedical ones and the reason is their high surface/volume ratio as well as their excellent optical properties and tunability. In this review article, we have summarized the results of studies on their thermal stability and the possibility of modifying the optical response of the particles by conventional and simple methods.

Author Contributions: Writing—original draft preparation, L.J.; writing—review and editing, Z.E., C.C. supervision, C.C. All authors have read and agreed to the published version of the manuscript.

Funding: Project no. TKP2021-NKTA-34 has been implemented with the support provided by the National Research, Development and Innovation Fund of Hungary, financed under the TKP2021-NKTA funding scheme. The work has been supported by the Development and Innovation Office NKFIH, Grant No.: OTKA.K143724.

Data Availability Statement: No new data were created or analyzed in this study. Data measured by the authors will be shared on request.

Acknowledgments: In this section you can acknowledge any support given which is not covered by the author contribution or funding sections. This may include administrative and technical support, or donations in kind (e.g., materials used for experiments).

Conflicts of Interest: The authors declare no conflict of interest.

References

1. Walter, P.; Welcomme, E.; Hallégot, P.; Zaluzec, N.J.; Deeb, C.; Castaing, J.; Veyssière, P.; Bréniaux, R.; Lévêque, J.L.; Tsoucaris, G. Early Use of PbS Nanotechnology for an Ancient Hair Dyeing Formula. *Nano Letters* **2006**, *6*, 2215–2219, [https://doi.org/10.1021/nl061493u]. PMID: 17034086, https://doi.org/10.1021/nl061493u.
2. Freestone, I.; Meeks, N.; Sax, M.; Higgitt, C. The Lycurgus Cup — A Roman nanotechnology. *Gold Bulletin* **2007**, *40*, 270–277. https://doi.org/10.1007/BF03215599.
3. Silva Ferreira, C.; de Castro Ribeiro, E.M.; Miranda Goes, A.d.; Mello Silva, B.d. Current strategies for diagnosis of paracoccidioidomycosis and prospects of methods based on gold nanoparticles. *Future Microbiology* **2016**, *11*, 973–985, [https://doi.org/10.2217/fmb-2016-0062]. PMID: 27416765, https://doi.org/10.2217/fmb-2016-0062.
4. Wang, C.; Zhang, H.; Zeng, D.; San, L.; Mi, X. DNA Nanotechnology Mediated Gold Nanoparticle Conjugates and Their Applications in Biomedicine. *Chinese Journal of Chemistry* **2016**, *34*, 299–307, [https://onlinelibrary.wiley.com/doi/pdf/10.1002/cjoc.20150083 https://doi.org/https://doi.org/10.1002/cjoc.201500839.

5. Comber, J.; Bamezai, A. Gold Nanoparticles (AuNPs): A New Frontier in Vaccine Delivery. *Journal of Nanomedicine Biotherapeutic Discovery* **2015**, *05*. https://doi.org/10.4172/2155-983X.1000e139.
6. Pasparakis, G. Light-Induced Generation of Singlet Oxygen by Naked Gold Nanoparticles and its Implications to Cancer Cell Phototherapy. *Small* **2013**, *9*, 4130–4134, [https://onlinelibrary.wiley.com/doi/pdf/10.1002/smll.201301365]. https://doi.org/https://doi.org/10.1002/smll.201301365.
7. Kirui, D.K.; Rey, D.A.; Batt, C.A. Gold hybrid nanoparticles for targeted phototherapy and cancer imaging. *Nanotechnology* **2010**, *21*, 105105. https://doi.org/10.1088/0957-4484/21/10/105105.
8. Chen, Q.; Chen, Q.; Qi, H.; Ruan, L.; Ren, Y. Experimental Comparison of Photothermal Conversion Efficiency of Gold Nanotriangle and Nanorod in Laser Induced Thermal Therapy. *Nanomaterials* **2017**, *7*. https://doi.org/10.3390/nano7120416.
9. Ahijado-Guzmán, R.; Sánchez-Arribas, N.; Martínez-Negro, M.; González-Rubio, G.; Santiago-Varela, M.; Pardo, M.; Piñeiro, A.; López-Montero, I.; Junquera, E.; Guerrero-Martínez, A. Intercellular Trafficking of Gold Nanostars in Uveal Melanoma Cells for Plasmonic Photothermal Therapy. *Nanomaterials* **2020**, *10*. https://doi.org/10.3390/nano10030590.
10. Jain, P.K.; Lee, K.S.; El-Sayed, I.H.; El-Sayed, M.A. Calculated Absorption and Scattering Properties of Gold Nanoparticles of Different Size, Shape, and Composition: Applications in Biological Imaging and Biomedicine. *The Journal of Physical Chemistry B* **2006**, *110*, 7238–7248. https://doi.org/10.1021/jp057170o.
11. Park, J.; Park, J.; Ju, E.J.; Park, S.S.; Choi, J.; Lee, J.H.; Lee, K.J.; Shin, S.H.; Ko, E.J.; Park, I.; et al. Multifunctional hollow gold nanoparticles designed for triple combination therapy and CT imaging. *Journal of Controlled Release* **2015**, *207*, 77–85. https://doi.org/https://doi.org/10.1016/j.jconrel.2015.04.007.
12. Kong, F.Y.; Zhang, J.W.; Li, R.F.; Wang, Z.X.; Wang, W.J.; Wang, W. Unique Roles of Gold Nanoparticles in Drug Delivery, Targeting and Imaging Applications. *Molecules* **2017**, *22*. https://doi.org/10.3390/molecules22091445.
13. Brown, S.D.; Nativo, P.; Smith, J.A.; Stirling, D.; Edwards, P.R.; Venugopal, B.; Flint, D.J.; Plumb, J.A.; Graham, D.; Wheate, N.J. Gold Nanoparticles for the Improved Anticancer Drug Delivery of the Active Component of Oxaliplatin. *Journal of the American Chemical Society* **2010**, *132*, 4678–4684, [https://doi.org/10.1021/ja908117a]. PMID: 20225865, https://doi.org/10.1021/ja908117a.
14. Khalil, I.; Julkapli, N.M.; Yehye, W.A.; Basirun, W.J.; Bhargava, S.K. Graphene–Gold Nanoparticles Hybrid—Synthesis, Functionalization, and Application in a Electrochemical and Surface-Enhanced Raman Scattering Biosensor. *Materials* **2016**, *9*. https://doi.org/10.3390/ma9060406.
15. Slavin, Y.N.; Asnis, J.; Häfeli, U.O.; Bach, H. Metal nanoparticles: understanding the mechanisms behind antibacterial activity. *Journal of Nanobiotechnology* **2017**, *15*, 65. https://doi.org/10.1186/s12951-017-0308-z.
16. Wriedt, T., Mie Theory: A Review. In *The Mie Theory: Basics and Applications*; Hergert, W.; Wriedt, T., Eds.; Springer Berlin Heidelberg: Berlin, Heidelberg, 2012; pp. 53–71. https://doi.org/10.1007/978-3-642-28738-1_2.
17. Mayer, K.M.; Hafner, J.H. Localized Surface Plasmon Resonance Sensors. *Chemical Reviews* **2011**, *111*, 3828–3857, [https://doi.org/10.1021/cr100313v]. PMID: 21648956, https://doi.org/10.1021/cr100313v.
18. Hu, S.; Tong, L.; Wang, J.; Yi, X.; Liu, J. NIR Light-Responsive Hollow Porous Gold Nanospheres for Controllable Pressure-Based Sensing and Photothermal Therapy of Cancer Cells. *Analytical Chemistry* **2019**, *91*, 15418–15424, [https://doi.org/10.1021/acs.analche 2 PMID: 31710205, https://doi.org/10.1021/acs.analchem.9b02871.
19. Hu, J.; Jiang, R.; Zhang, H.; Guo, Y.; Wang, J.; Wang, J. Colloidal porous gold nanoparticles. *Nanoscale* **2018**, *10*, 18473–18481. https://doi.org/10.1039/C8NR06149A.
20. Wang, D.; Ji, R.; Albrecht, A.; Schaaf, P. Ordered arrays of nanoporous gold nanoparticles. *Beilstein Journal of Nanotechnology* **2012**, *3*, 651–657. https://doi.org/10.3762/bjnano.3.74.
21. Pedireddy, S.; Lee, H.K.; Tjiu, W.W.; Phang, I.Y.; Tan, H.R.; Chua, S.Q.; Troadec, C.; Ling, X.Y. One-step synthesis of zero-dimensional hollow nanoporous gold nanoparticles with enhanced methanol electrooxidation performance. *Nature Communications* **2014**, *5*, 4947. https://doi.org/10.1038/ncomms5947.
22. Schmidl, G.; Raugust, M.; Jia, G.; Dellith, A.; Dellith, J.; Schmidl, F.; Plentz, J. Porous spherical gold nanoparticles via a laser induced process. *Nanoscale Adv.* **2022**, *4*, 4122–4130. https://doi.org/10.1039/D2NA00396A.
23. Wang, D.; Schaaf, P. Nanoporous gold nanoparticles. *J. Mater. Chem.* **2012**, *22*, 5344–5348. https://doi.org/10.1039/C2JM15727F.
24. Thompson, C.V. Solid-State Dewetting of Thin Films. *Annual Review of Materials Research* **2012**, *42*, 399–434, [https://doi.org/10.1146/matsci-070511-155048]. https://doi.org/10.1146/annurev-matsci-070511-155048.
25. McCue, I.; Benn, E.; Gaskey, B.; Erlebacher, J. Dealloying and Dealloyed Materials. *Annual Review of Materials Research* **2016**, *46*, 263–286, [https://doi.org/10.1146/annurev-matsci-070115-031739]. https://doi.org/10.1146/annurev-matsci-070115-031739.
26. Kosinova, A.; Wang, D.; Schaaf, P.; Kovalenko, O.; Klinger, L.; Rabkin, E. Fabrication of hollow gold nanoparticles by dewetting, dealloying and coarsening. *Acta Materialia* **2016**, *102*, 108–115. https://doi.org/https://doi.org/10.1016/j.actamat.2015.09.024.
27. Wang, D.; Schaaf, P. Nanoporous gold nanoparticles. *J. Mater. Chem.* **2012**, *22*, 5344–5348. https://doi.org/10.1039/C2JM15727F.
28. Xiao, S.; Wang, S.; Wang, X.; Xu, P. Nanoporous gold: A review and potentials in biotechnological and biomedical applications. *Nano Select*, *n/a*, [https://onlinelibrary.wiley.com/doi/pdf/10.1002/nano.202000291]. https://doi.org/https://doi.org/10.1002/nano.202000291.
29. Biener, M.M.; Biener, J.; Wichmann, A.; Wittstock, A.; Baumann, T.F.; Bäumer, M.; Hamza, A.V. ALD Functionalized Nanoporous Gold: Thermal Stability, Mechanical Properties, and Catalytic Activity. *Nano Letters* **2011**, *11*, 3085–3090, [https://doi.org/10.1021/nl200993g]. PMID: 21732623, https://doi.org/10.1021/nl200993g.

 doi:10.20944/preprints202306.0324.v1

30. Jia, C.; Yin, H.; Ma, H.; Wang, R.; Ge, X.; Zhou, A.; Xu, X.; Ding, Y. Enhanced Photoelectrocatalytic Activity of Methanol Oxidation on TiO2-Decorated Nanoporous Gold. *The Journal of Physical Chemistry C* **2009**, *113*, 16138–16143, [https://doi.org/10.1021/jp904191k]. https://doi.org/10.1021/jp904191k.
31. Atta, S.; Pennington, A.M.; Celik, F.E.; Fabris, L. TiO2 on Gold Nanostars Enhances Photocatalytic Water Reduction in the Near-Infrared Regime. *Chem* **2018**, *4*, 2140–2153. https://doi.org/https://doi.org/10.1016/j.chempr.2018.06.004.
32. Lee, J.; Lee, S.J.; Han, W.B.; Jeon, H.; Park, J.; Jang, W.; Yoon, C.S.; Jeon, H. Deposition temperature dependence of titanium oxide thin films grown by remote-plasma atomic layer deposition. *physica status solidi (a)* **2013**, *210*, 276–284, [https://onlinelibrary.wiley.com/doi/pdf/10.1002/pssa.201228671]. https://doi.org/https://doi.org/10.1002/pssa.201228671.
33. Hussien, M.S.; Shenouda, S.; Parditka, B.; Csík, A.; Erdélyi, Z. Enhancement of Urbach's energy and non-lattice oxygen content of TiO1.7 ultra-thin films for more photocatalytic activity. *Ceramics International* **2020**, *46*, 15236–15241. https://doi.org/https://doi.org/10.1016/j.ceramint.2020.03.062.
34. Avila, J.R.; Qadri, S.B.; Freitas, J.A.; Nepal, N.; Boris, D.R.; Walton, S.G.; Eddy, C.R.; Wheeler, V.D. Impact of Growth Conditions on the Phase Selectivity and Epitaxial Quality of TiO2 Films Grown by the Plasma-Assisted Atomic Layer Deposition. *Chemistry of Materials* **2019**, *31*, 3900–3908, [https://doi.org/10.1021/acs.chemmater.8b05282]. https://doi.org/10.1021/acs.chemmater.8b05282.
35. Kosinova, A.; Wang, D.; Baradács, E.; Parditka, B.; Kups, T.; Klinger, L.; Erdélyi, Z.; Schaaf, P.; Rabkin, E. Tuning the nanoscale morphology and optical properties of porous gold nanoparticles by surface passivation and annealing. *Acta Materialia* **2017**, *127*, 108–116. https://doi.org/https://doi.org/10.1016/j.actamat.2017.01.014.
36. Juhász, L.; Parditka, B.; Shanda Shenouda, S.; Kadoi, M.; Fukunaga, K.i.; Erdélyi, Z.; Cserháti, C. Morphological and in situ local refractive index change induced tuning of the optical properties of titania coated porous gold nanoparticles. *Journal of Applied Physics* **2020**, *128*, 054303, [https://doi.org/10.1063/5.0010460]. https://doi.org/10.1063/5.0010460.
37. Awazu, K.; Fujimaki, M.; Rockstuhl, C.; Tominaga, J.; Murakami, H.; Ohki, Y.; Yoshida, N.; Watanabe, T. A Plasmonic Photocatalyst Consisting of Silver Nanoparticles Embedded in Titanium Dioxide. *Journal of the American Chemical Society* **2008**, *130*, 1676–1680, [https://doi.org/10.1021/ja076503n]. PMID: 18189392, https://doi.org/10.1021/ja076503n.
38. Garcia, M.A. Surface plasmons in metallic nanoparticles: fundamentals and applications. *Journal of Physics D: Applied Physics* **2011**, *44*, 283001. https://doi.org/10.1088/0022-3727/44/28/283001.
39. Ozbay, E. Plasmonics: Merging Photonics and Electronics at Nanoscale Dimensions. *Science* **2006**, *311*, 189–193, [https://science.sciencemag.org/content/311/5758/189.full.pdf]. https://doi.org/10.1126/science.1114849.
40. Fritzsche, W.; Taton, T.A. Metal nanoparticles as labels for heterogeneous, chip-based DNA detection. *Nanotechnology* **2003**, *14*, R63–R73. https://doi.org/10.1088/0957-4484/14/12/r01.
41. Huang, X.; El-Sayed, M.A. Gold nanoparticles: Optical properties and implementations in cancer diagnosis and photothermal therapy. *Journal of Advanced Research* **2010**, *1*, 13–28. https://doi.org/https://doi.org/10.1016/j.jare.2010.02.002.
42. Sztandera, K.; Gorzkiewicz, M.; Klajnert-Maculewicz, B. Gold Nanoparticles in Cancer Treatment. *Molecular Pharmaceutics* **2019**, *16*, 1–23, [https://doi.org/10.1021/acs.molpharmaceut.8b00810]. PMID: 30452861, https://doi.org/10.1021/acs.molpharmaceut.8b00810.
43. Safwat, M.A.; Soliman, G.M.; Sayed, D.; Attia, M.A. Fluorouracil-Loaded Gold Nanoparticles for the Treatment of Skin Cancer: Development, in Vitro Characterization, and in Vivo Evaluation in a Mouse Skin Cancer Xenograft Model. *Molecular Pharmaceutics* **2018**, *15*, 2194–2205, [https://doi.org/10.1021/acs.molpharmaceut.8b00047]. PMID: 29701979, https://doi.org/10.1021/acs.molpharmaceut.8b00047.
44. Majidi, F.S.; Mohammadi, E.; Mehravi, B.; Nouri, S.; Ashtari, K.; Neshasteh-riz, A. Investigating the effect of near infrared photo thermal therapy folic acid conjugated gold nano shell on melanoma cancer cell line A375. *Artificial Cells, Nanomedicine, and Biotechnology* **2019**, *47*, 2161–2170, [https://doi.org/10.1080/21691401.2019.1593188]. PMID: 31159585, https://doi.org/10.1080/21691401.2019.1593188.
45. Hainfeld, J.F.; O'Connor, M.J.; Lin, P.; Qian, L.; Slatkin, D.N.; Smilowitz, H.M. Infrared-Transparent Gold Nanoparticles Converted by Tumors to Infrared Absorbers Cure Tumors in Mice by Photothermal Therapy. *PLOS ONE* **2014**, *9*, 1–11. https://doi.org/10.1371/journal.pone.0088414.
46. Bedford, E.E.; Spadavecchia, J.; Pradier, C.M.; Gu, F.X. Surface Plasmon Resonance Biosensors Incorporating Gold Nanoparticles. *Macromolecular Bioscience* **2012**, *12*, 724–739, [https://onlinelibrary.wiley.com/doi/pdf/10.1002/mabi.201100435]. https://doi.org/https://doi.org/10.1002/mabi.201100435.
47. Amendola, V.; Pilot, R.; Frasconi, M.; Maragò, O.M.; Iatì, M.A. Surface plasmon resonance in gold nanoparticles: a review. *Journal of Physics: Condensed Matter* **2017**, *29*, 203002. https://doi.org/10.1088/1361-648x/aa60f3.
48. Rao, W.; Wang, D.; Kups, T.; Baradács, E.; Parditka, B.; Erdélyi, Z.; Schaaf, P. Nanoporous Gold Nanoparticles and Au/Al2O3 Hybrid Nanoparticles with Large Tunability of Plasmonic Properties. *ACS Applied Materials & Interfaces* **2017**, *9*, 6273–6281, [https://doi.org/10.1021/acsami.6b13602]. PMID: 28145115, https://doi.org/10.1021/acsami.6b13602.
49. Juhász, L.; Parditka, B.; Petrik, P.; Cserháti, C.; Erdélyi, Z. Continuous tuning of the plasmon resonance frequency of porous gold nanoparticles by mixed oxide layers. *Journal of Porous Materials* **2020**, *27*, 1583–1588. https://doi.org/10.1007/s10934-020-00933-w.
50. Juhász, L.; Moldován, K.; Herman, P.; Erdélyi, Z.; Fábián, I.; Kalmár, J.; Cserháti, C. Synthesis and Stabilization of Support-Free Mesoporous Gold Nanoparticles. *Nanomaterials* **2020**, *10*. https://doi.org/10.3390/nano10061107.

 doi:10.20944/preprints202306.0324.v1